Multidisciplinary ⋮ Rapid Review ⋮ Open Access Journal

Digital Object Identifier

Effective Capacity Analysis over Generalized Composite Fading Channels

SEONG KI YOO[1], (Member, IEEE), SIMON L. COTTON[2], (Senior Member, IEEE), PASCHALIS C. SOFOTASIOS[3, 4], (Senior Member, IEEE), SAMI MUHAIDAT[4], (Senior Member, IEEE), and GEORGE K. KARAGIANNIDIS[5], (Fellow Member, IEEE)

[1]Centre for Data Science, Faculty of Engineering, Environment and Computing, Coventry University, UK, CV1 2TL (e-mail: ad3869@coventry.ac.uk)
[2]Centre for Wireless Innovation, ECIT Institute, Queen's University Belfast, UK, BT3 9DT (e-mail: simon.cotton@qub.ac.uk)
[3]Department of Electronics and Communications Engineering, Tampere University of Technology, Tampere 33101, Finland (e-mail: p.sofotasios@ieee.org)
[4]Center for Cyber-Physical Systems, Department of Electrical Engineering and Computer Science, Khalifa University of Science and Technology, Abu Dhabi 127788, UAE (e-mail: muhaidat@ieee.org)
[5]Department of Electrical and Computer Engineering, Aristotle University of Thessaloniki, 54 124 Thessaloniki, Greece (email: geokarag@auth.gr)

This work was supported in part by the U.K. Engineering and Physical Sciences Research Council under Grant No. EP/L026074/1 and the Department for the Economy Northern Ireland through Grant No. USI080.

ABSTRACT A performance analysis of the effective capacity in two recently proposed generalized composite fading channels, namely κ-μ / inverse gamma and η-μ / inverse gamma composite fading channels, is conducted. To this end, accurate analytic expressions for the effective capacity are derived along with simple tight bound representations. Additionally, simple approximate expressions at the high average signal-to-noise ratio regime are also provided. The effective capacity is then analyzed for different delay constraint, multipath fading and shadowing conditions. The numerical results show that the achievable spectral efficiency lessens as the multipath fading and shadowing parameters decrease (i.e., severe multipath fading and heavy shadowing become prevalent) or the delay constraint increases. The accuracy and tightness of the proposed bounds is demonstrated and approximate representations are also provided to verify their usefulness. Furthermore, our numerical results are validated through a careful comparison with the simulated results.

INDEX TERMS Channel capacity, composite fading, effective capacity, η-μ / inverse gamma model, κ-μ / inverse gamma model.

I. INTRODUCTION

CHANNEL capacity is a core performance metric in communication systems. Shannon's ergodic capacity has widely been used, but this is not able to measure the system performance under quality of service (QoS) constraints such as system delay and data rate. Effective capacity has been proposed as an alternative performance metric owing to its ability to take into account the system's delay constraint [1]. This is especially pertinent for emerging real-time, delay sensitive applications where the lowest possible latency is essential. Additionally, computation of the effective capacity offers an efficient and convenient way to evaluate the statistical QoS performance of wireless systems from the networking perspective. This includes the analysis of resource allocation management [2], spectral efficiency [3], user scheduling schemes [4] and cognitive radio networks [5]. Due to the aforementioned attractions, the effective capacity has recently attracted significant research interest.

Similar to other capacity measures, the effective capacity is also greatly impacted by the fading conditions experienced within the operating environment. In this context, the effective capacity has been determined over a number of different multipath fading [6]–[13] and composite fading channels [14]–[20]. For example, the authors of [6] evaluated the effective capacity of Nakagami-m fading channels. This was then extended in [7] to account for the case of multiple-input single-output (MISO) fading channels. In this study, a comprehensive analysis of the effective rate over independent and identically distributed (i.i.d.) Nakagami-m fading channels was conducted. Meanwhile, in [15], the authors presented an exact closed-form expression for the effective capacity of $\mathcal{F}$ composite fading channels as well as demonstrating the effect of different shadowing and multipath fading conditions on the effective capacity.

More recently, two generalized composite fading models have been introduced in [21], namely the κ-μ / inverse gamma and η-μ / inverse gamma composite fading models. The former characterizes the composite fading observed in

This article has been accepted for publication in a future issue of this journal, but has not been fully edited. Content may change prior to final publication. Citation information: DOI 10.1109/ACCESS.2020.3003207, IEEE Access

line-of-sight channel conditions whereas the latter accounts for the composite fading experienced in non-line-of-sight channel conditions. In [21], the authors demonstrated their utility for channel characterization in wearable, cellular and vehicular communications. To the best of the author's knowledge, a detailed mathematical treatment of the effective capacity over these two generalized composite fading channels has not been presented in open technical literature. To this end, using a similar approach to that utilized in [22], we firstly reformulate the corresponding probability density functions (PDFs) to ensure stability across the complete parameter space when conducting calculations which involve computation of the moments. We then derive accurate analytic expressions and tight bounds for the effective capacity. Additionally, simple approximate expressions at the high average signal-to-noise ratio (SNR) regime are also derived. Using the newly obtained expressions, we provide important insights into the impact of delay constraint, multipath fading and shadowing on the effective capacity under generalized composite fading conditions.

II. THE κ-μ / INVERSE GAMMA COMPOSITE FADING MODEL

A. A NEW FORMULATION

Similar to the κ-μ fading model [23], the κ-μ / inverse gamma composite fading model describes a fading scenario in which the radio channel exhibits multipath clustering with presence of dominant components. Unlike the κ-μ fading channel, however, in the κ-μ / inverse gamma composite fading channel, the mean signal power of a κ-μ signal is assumed to be randomly fluctuated by an inverse gamma random variable (RV). Following this definition, the composite signal envelope, R, in a κ-μ / inverse gamma composite fading channel can be defined as

$$R^2 = \sum_{i=1}^{n} Z(X_i + p_i)^2 + Z(Y_i + q_i)^2 \tag{1}$$

where n represents the number of multipath clusters, X_i and Y_i are mutually independent Gaussian RVs with $\mathbb{E}[X_i] = \mathbb{E}[Y_i] = 0$ and $\mathbb{E}\left[X_i^2\right] = \mathbb{E}\left[Y_i^2\right] = \sigma^2$ where $\mathbb{E}[\cdot]$ denotes the statistical expectation. Additionally, p_i and q_i are the mean values of the in-phase and quadrature components of the multipath cluster i, respectively, which yields $\delta^2 = \sum_{i=1}^{n} p_i^2 + q_i^2$ with δ^2 denoting the total power of the dominant signal components. In (1), Z denotes an inverse gamma RV with $\mathbb{E}[Z] = 1$, where m_s is the shape parameter and thus the corresponding PDF of Z is given by

$$f_Z(\zeta) = \frac{(m_s - 1)^{m_s}}{\Gamma(m_s)\,\zeta^{m_s+1}} \exp\left(-\frac{m_s - 1}{\zeta}\right) \tag{2}$$

where $\Gamma(\cdot)$ denotes the gamma function.

Theorem 1. *For $\kappa, \mu, r, \Omega, m_s \in \mathbb{R}^+$, the PDF of the composite signal envelope in a κ-μ / inverse gamma composite fading channel can be expressed in closed-form as*

$$f_R(r) = \frac{2\mu^{\mu}(1+\kappa)^{\mu}(m_s-1)^{m_s}\Omega^{m_s} r^{2\mu-1}}{\exp(\mu\kappa)\,B(m_s,\mu)\,c_0^{\,m_s+\mu}} \times {}_1F_1\left(m_s+\mu;\mu;\frac{\mu^2\kappa(1+\kappa)\,r^2}{c_0}\right),\ m_s > 1 \tag{3}$$

where $c_0 = \mu(1+\kappa)\,r^2 + (m_s-1)\Omega$. In (3), $B(\cdot,\cdot)$ denotes the Beta function [24] while ${}_1F_1(\cdot;\cdot;\cdot)$ represents the Kummer hypergeometric function [24].

Proof. The PDF of the signal envelope in a κ-μ / inverse gamma composite channel can be obtained by averaging the infinite integral of the conditional probability density of the κ-μ fading process with respect to the random variation of the mean signal power, such that

$$f_R(r) = \int_0^{\infty} f_{R|Z}(r|\zeta) f_Z(\zeta)\, d\zeta \tag{4}$$

where

$$f_{R|Z}(r|\zeta) = \frac{2\mu(1+\kappa)^{\frac{\mu+1}{2}} r^{\mu}}{\kappa^{\frac{\mu-1}{2}} \exp(\mu\kappa)(\zeta\Omega)^{\frac{\mu+1}{2}}} \exp\left(-\mu(1+\kappa)\frac{r^2}{\zeta\Omega}\right) \times I_{\mu-1}\left(2\mu\sqrt{\kappa(1+\kappa)}\frac{r}{\sqrt{\zeta\Omega}}\right) \tag{5}$$

where $I_v(\cdot)$ denotes the modified Bessel function of the first kind and order v [25, Eq. (9.6.20)]. Substituting (5) and (2) in (4), performing a simple transformation of variables and applying [26, Eq. (2.15.5.4)] along with some algebraic manipulations, the PDF of the κ-μ / inverse gamma composite fading model can be expressed in closed-form as given in (3). □

The *doubly* non-central $\mathcal{F}$ distribution arises as a result of the ratio of two independent distributed non-central chi-squared variables [27], i.e., $\chi^2_{v_1}(\lambda_1)$ and $\chi^2_{v_2}(\lambda_2)$. This simplifies to the $\mathcal{F}$ distribution when $\lambda_1 = \lambda_2 = 0$ and the *singly* non-central $\mathcal{F}$ distribution when $\lambda_1 \neq 0, \lambda_2 = 0$. Interestingly, the form of the PDF in (3) corresponds to the *singly* non-central $\mathcal{F}$ distribution. More specifically, when letting $r^2 = t$ and then performing the requisite transformation along with the following substitutions $\mu = v_1/2, m_s = v_2/2, \kappa = \lambda/v_1$ and $\Omega = v_2(v_1+\lambda)/v_1(v_2-2)$, the *singly* non-central $\mathcal{F}$ distribution, $f_t(t)$, can obtained with parameters v_1, v_2 and λ.

Remark 1. *Physically, μ is related to the number of multipath clusters while $\kappa = \frac{\delta^2}{2\mu\sigma^2}$ parameter represents the ratio between the total power of the dominant signal and scattered signal components ($2\mu\sigma^2$) [1]. In this model, m_s controls the amount of shadowing of the mean signal power ($\Omega = \mathbb{E}[R^2] = \delta^2 + 2\mu\sigma^2$) undergoes.*

The corresponding PDF of the instantaneous signal-to-noise ratio (SNR) can be obtained from (3) by letting $\gamma = \overline{\gamma} r^2/\Omega$,

[1] Each cluster is assumed to have the scattered wave with identical power, i.e., $2\sigma^2$

This article has been accepted for publication in a future issue of this journal, but has not been fully edited. Content may change prior to final publication. Citation information: DOI 10.1109/ACCESS.2020.3003207, IEEE Access

such that

$$f_\gamma(\gamma) = \frac{\mu^\mu (1+\kappa)^\mu (m_s-1)^{m_s} \overline{\gamma}^{m_s} \gamma^{\mu-1}}{\exp(\mu\kappa)\, B(m_s,\mu)\, {c_1}^{m_s+\mu}} \times {}_1F_1\left(m_s+\mu;\mu;\frac{\mu^2\kappa(1+\kappa)\gamma}{c_1}\right) \tag{6}$$

where $c_1 = \mu(1+\kappa)\gamma + (m_s-1)\overline{\gamma}$ and $\overline{\gamma} = \mathbb{E}[\gamma]$ is the average SNR.

B. EFFECTIVE CAPACITY

Theorem 2. *For $\kappa, \mu, \overline{\gamma}, \theta, B, T \in \mathbb{R}^+$ and $m_s > 1$, the following analytic expression holds for the effective capacity over κ-μ / inverse gamma composite fading channels*

$$C_E = -\frac{1}{A}\log_2\left\{\frac{(m_s)_A\, {c_2}^{m_s}}{\exp(\mu\kappa)} \sum_{i=0}^{\infty} \frac{(\mu\kappa)^i}{i!\,(m_s+\mu+i)_A} \times {}_2F_1\Big(m_s+A, m_s+\mu+i; m_s+\mu+i+A; 1-c_2\Big)\right\} \tag{7}$$

where $c_2 = \dfrac{(m_s-1)\overline{\gamma}}{\mu(1+\kappa)}$ and $A = \theta BT/\ln(2)$ with θ denoting the asymptotic decay rate of the buffer occupancy. It is worth remarking that when $\theta \to 0$ (i.e., no delay constraints), the effective capacity coincides with the well-known Shannon's ergodic capacity whereas the effective capacity deteriorates to zero when $\theta \to \infty$ (i.e., severely delay-limited case). Additionally, B refers to the system bandwidth while T represents the block/frame length. In (7)*, $(x)_n$ denotes the Pochhammer symbol [24] while ${}_2F_1(\cdot,\cdot;\cdot;\cdot)$ represents the Gauss hypergeometric function [24].*

Proof. Based on the definition of effective capacity given in [14], the effective capacity can be defined as

$$C_E = -\frac{1}{A}\log_2\left(\mathbb{E}\left[(1+\gamma)^{-A}\right]\right). \tag{8}$$

Considering a κ-μ / inverse gamma composite fading channel, we can calculate the effective capacity from (8) by averaging the SNR, γ, with the PDF given in (6), such that

$$C_E = -\frac{1}{A}\log_2\left(\frac{\mu^\mu(1+\kappa)^\mu(m_s-1)^{m_s}\overline{\gamma}^{m_s}}{\exp(\mu\kappa)\, B(m_s,\mu)}\mathcal{I}_1\right) \tag{9}$$

where

$$\mathcal{I}_1 = \int_0^\infty \frac{(1+\gamma)^{-A}\gamma^{\mu-1}}{{c_1}^{m_s+\mu}} {}_1F_1\left(m_s+\mu;\mu;\frac{\mu^2\kappa(1+\kappa)\gamma}{c_1}\right). \tag{10}$$

The Kummer hypergeometric function in (10) can be expressed in terms of an infinite series expansion [28, Eq. (07.20.02.0001.01)]. With the aid of [24, Eq. (3.197.9)], we can then obtain the following expression

$$C_E = -\frac{1}{A}\log_2\left\{\sum_{i=0}^{\infty}\frac{(m_s+\mu)_i\, {c_2}^{m_s} B(m_s+A,\mu+i)}{i!\,(\mu)_i(\mu\kappa)^{-i}\exp(\mu\kappa)\, B(m,m_s)} \times {}_2F_1\Big(m_s+A, m_s+\mu+i; m_s+\mu+i+A; 1-c_2\Big)\right\}. \tag{11}$$

The effective capacity expression given in (11) can be expressed in a more compact form by rewriting the Pochhammer symbol and beta function in terms of the gamma function along with some algebraic manipulations. This completes the proof. □

Proposition 1. *For $\kappa, \mu, \overline{\gamma}, \theta, B, T \in \mathbb{R}^+$ and $m_s > 1$, the following upper bound is valid for the truncation error of* (7)*,*

$$\mathcal{T} \le -\frac{1}{A}\log_2\left\{\frac{(m_s)_A\, {c_2}^{m_s}}{(c_3)_A} {}_2F_1\Big(m_s+A, c_3; c_3+A; 1-c_2\Big)\right\} \tag{12}$$

where $c_3 = m_s+\mu+p$ with p denoting the number of terms that truncate the series.

Proof. Truncating the infinite series in (7) after $p-1$ terms results in the following error

$$\mathcal{T} = -\frac{1}{A}\log_2\left\{\frac{(m_s)_A\, {c_2}^{m_s}}{\exp(\mu\kappa)} \sum_{i=p}^{\infty} \frac{(\mu\kappa)^i}{i!\,(m_s+\mu+i)_A} \times {}_2F_1\Big(m_s+A, m_s+\mu+i; m_s+\mu+i+A; 1-c_2\Big)\right\}. \tag{13}$$

Since the gamma and Gauss hypergeometric functions in (13) are monotonically decreasing with respect to i, $\mathcal{T}$ can be bounded as

$$\mathcal{T} \le -\frac{1}{A}\log_2\left\{\frac{{}_2F_1\Big(m_s+A, c_3; c_3+A; 1-c_2\Big)(m_s)_A}{{c_2}^{-m_s}\exp(\mu\kappa)\,(c_3)_A} \times \sum_{i=p}^{\infty}\frac{(\mu\kappa)^i}{i!}\right\}. \tag{14}$$

The limits of the summation in (14) can be rewritten as $\sum_{i=p}^{\infty}\frac{(\mu\kappa)^i}{i!} \le \sum_{i=0}^{\infty}\frac{(\mu\kappa)^i}{i!}$ as the positive terms are only added up. Notably, by using $\sum_{i=0}^{\infty}\frac{(\mu\kappa)^i}{i!} = \exp(\mu\kappa)$, we can obtain (12), which completes the proof. □

Proposition 2. *For $\kappa, \mu, \overline{\gamma}, \theta, B, T \in \mathbb{R}^+$, $m_s > 1$ and $m_s + \mu \gg A$, the effective capacity under κ-μ / inverse gamma composite fading conditions can be bounded by the following inequalities*

$$C_E^{UB} < -\frac{1}{A}\log_2\left[\frac{(m_s)_A}{{c_2}^A\,(m_s+\mu+p)_A}\right] \tag{15}$$

and

$$C_E^{LB} > -\frac{1}{A}\log_2\left[\frac{(m_s)_A}{{c_2}^A}\right] \tag{16}$$

which represent tight upper and lower bounds, respectively.

This article has been accepted for publication in a future issue of this journal, but has not been fully edited. Content may change prior to final publication. Citation information: DOI 10.1109/ACCESS.2020.3003207, IEEE Access

Proof. It is evident that $m_s+\mu+A \approx m_s+\mu$ when $m_s+\mu >> A$ and thus (7) can be tightly upper bounded

$$C_E^{UB} < -\frac{1}{A}\log_2\Bigg\{\frac{(m_s)_A\, c_2^{m_s}}{\exp(\mu\kappa)}\sum_{i=0}^{\infty}\frac{(\mu\kappa)^i}{i!\,(m_s+\mu+i)_A} \times {}_2F_1\Big(m_s+A, m_s+\mu+i; m_s+\mu+i; 1-c_2\Big)\Bigg\}. \tag{17}$$

Given that ${}_2F_1(m_s+A, m_s+\mu+i; m_s+\mu+i; 1-c_2) = {}_1F_0(m_s+A; ; 1-c_2)$ with ${}_1F_0(\cdot;;\cdot)$ denoting the Generalized hypergeometric function [24, Eq. (9.14.1)] and by recalling that ${}_1F_0(n; ; 1+x) \triangleq (-1)^n/x^n$, $n \in \mathbb{R}$, (17) can be reduced as follows

$$C_E^{UB} < -\frac{1}{A}\log_2\left[\frac{(m_s)_A}{\exp(\mu\kappa)\, c_2{}^A}\sum_{i=0}^{\infty}\frac{(\mu\kappa)^i}{i!\,(m_s+\mu+i)_A}\right]. \tag{18}$$

After some algebraic manipulations, the closed-form upper bound is deduced as given in (15).

Based on (15) and recalling that $m_s+\mu+A \approx m_s+\mu$ when $m_s+\mu \gg A$, $(m_s+\mu+p)_A$ in (15) can be eliminated. This yields the closed-form lower bound as given in (16), which completes the proof. □

Although (7) provides an accurate expression for calculating the effective capacity in κ-μ / inverse gamma composite fading channels across all SNR values, in what follows, we present a useful and simplified asymptotic expression for high SNR regimes.

Proposition 3. *For $\kappa, \mu, \overline{\gamma}, \theta, B, T \in \mathbb{R}^+$, $m_s > 1$ and $\overline{\gamma} \gg 0$, the effective capacity under κ-μ / inverse gamma composite fading conditions can be asymptotically expressed as follows*

$$C_E^{asym.} \simeq -\frac{1}{A}\log_2\Big[{}_2F_1(A, \mu+p; c_3+A; 1-\overline{\gamma})\Big]. \tag{19}$$

Proof. In the high average SNR regime ($\overline{\gamma} \gg 0$), it follows that $\overline{\gamma} \gg \kappa$, $\overline{\gamma} \gg \mu$, $\overline{\gamma} \gg m_s$ and $\overline{\gamma} \gg A$, namely

$$\frac{(m_s)_A}{(m_s+\mu+i)_A}\left(\frac{(m_s-1)\overline{\gamma}}{\mu(1+\kappa)}\right)^{m_s} \simeq \overline{\gamma}^{\,m_s}. \tag{20}$$

Based on this and after some algebraic manipulations, (19) is deduced, which completes the proof. □

III. THE η-μ / INVERSE GAMMA COMPOSITE FADING MODEL

A. A NEW FORMULATION

Similar to the η-μ fading model [23], the η-μ / inverse gamma composite fading model describes the variation of the fading signal with power imbalance or correlation between its quadrature components and multipath clusters. Unlike the η-μ fading channel, however, in the η-μ / inverse gamma fading channel, the mean signal power of an η-μ signal is assumed to be randomly fluctuated by an inverse gamma RV. The corresponding composite signal envelope in an η-μ / inverse gamma composite fading channel can be written as

$$R^2 = \sum_{i=1}^{n} ZX_i^2 + ZY_i^2 \tag{21}$$

where n denotes the number of multipath clusters and Z represents an inverse gamma RV with $\mathbb{E}[Z]=1$ whose PDF is given in (2). In *Format* 1, X_i and Y_i are mutually independent Gaussian RVs with $\mathbb{E}[X_i] = \mathbb{E}[Y_i] = 0$, $\mathbb{E}\left[X_i^2\right] = \sigma_X^2$ and $\mathbb{E}\left[Y_i^2\right] = \sigma_Y^2$, while in *Format* 2, X_i and Y_i are mutually correlated Gaussian RVs with $\mathbb{E}[X_i] = \mathbb{E}[Y_i] = 0$, and $\mathbb{E}\left[X_i^2\right] = \mathbb{E}\left[Y_i^2\right] = \sigma^2$.

Theorem 3. *For $\eta, \mu, r, \Omega, m_s \in \mathbb{R}^+$ and $m_s > 1$, the PDF of the composite signal envelope in an η-μ / inverse gamma composite fading channel can be written as*

$$f_R(r) = \frac{2^{2\mu+1}\mu^{2\mu}\, h^{\mu}(m_s-1)^{m_s}\Omega^{m_s} r^{4\mu-1}}{B(m_s, 2\mu)[2\mu h r^2 + (m_s-1)\Omega]^{m_s+2\mu}} \times {}_2F_1\left(\frac{m_s+2\mu}{2}, \frac{m_s+2\mu+1}{2}; \mu+\frac{1}{2}; \frac{\left(2\mu H r^2\right)^2}{\left[2\mu h r^2+(m_s-1)\Omega\right]^2}\right) \tag{22}$$

where $h = (2+\eta^{-1}+\eta)/4$, $H = (\eta^{-1}-\eta)/4$ in Format 1 and $h = 1/(1-\eta^2)$, $H = \eta/(1-\eta^2)$ in Format 2.

Proof. Based on the signal model given in (21), the conditional probability density of the η-μ fading process with respect to the random variation of the mean signal power can be expressed as follows

$$f_{R|Z}(r|\zeta) = \frac{4\sqrt{\pi}\,\mu^{\mu+\frac{1}{2}}\, h^{\mu} r^{2\mu}}{\Gamma(\mu)\, H^{\mu-\frac{1}{2}}(\zeta\Omega)^{\mu+\frac{1}{2}}} \times \exp\left(-\frac{2\mu h r^2}{\zeta\Omega}\right) I_{\mu-\frac{1}{2}}\left(\frac{2\mu H r^2}{\zeta\Omega}\right). \tag{23}$$

By substituting (23) and (2) into (4), performing a simple transformation of variables and applying [26, Eq. (2.15.3.2)] along with some algebraic manipulations, the corresponding PDF of the composite fading signal in an η-μ / inverse gamma composite fading channel can be expressed in closed-form as given in (22). □

Remark 2. *Physically, μ is related to the number of multipath clusters and η is defined as the ratio between the scattered wave power of the in-phase and quadrature components of each multipath cluster ($\eta = \sigma_I^2/\sigma_Q^2$) in Format 1. On the contrary, in Format 2, η is defined as the correlation coefficient between the scattered waves in the in-phase and quadrature components of each multipath cluster ($\eta = \mathbb{E}[I_i Q_i]/\sigma^2$). In this model, the m_s parameter controls the amount of shadowing of the mean signal power, i.e., $\mathbb{E}\left[R^2\right] = \Omega = \mu(1+\eta)\,\sigma_Q^2 = \mu\left(1+\eta^{-1}\right)\sigma_I^2$ in Format 1 and $\mathbb{E}\left[R^2\right] = \Omega = 2\mu\sigma^2$ in Format 2.*

This article has been accepted for publication in a future issue of this journal, but has not been fully edited. Content may change prior to final publication. Citation information: DOI 10.1109/ACCESS.2020.3003207, IEEE Access

The corresponding PDF of the instantaneous SNR can be obtained from (22) by letting $\gamma = \overline{\gamma} r^2/\Omega$, such that

$$f_\gamma(\gamma) = \frac{2^{2\mu}\mu^{2\mu}\, h^\mu (m_s-1)^{m_s}\overline{\gamma}^{m_s}\gamma^{2\mu-1}}{B(m_s,2\mu)\, {c_4}^{m_s+2\mu}} \times {}_2F_1\left(\frac{m_s+2\mu}{2}, \frac{m_s+2\mu+1}{2}; \mu+\frac{1}{2}; \frac{(2\mu H\gamma)^2}{{c_4}^2}\right) \tag{24}$$

where $c_4 = 2\mu h\gamma + (m_s-1)\overline{\gamma}$.

B. EFFECTIVE CAPACITY

Theorem 4. *For $\mu, \overline{\gamma}, \theta, B, T \in \mathbb{R}^+$, $m_s > 1$, $\eta \in \mathbb{R}^+$ in Format 1 and $-1 < \eta < 1$ in Format 2, the following analytic expression holds for the effective capacity in η-μ / inverse gamma composite fading channels*

$$C_E = -\frac{1}{A}\log_2\left\{\sum_{i=0}^{\infty}\frac{(\mu)_i\,(m_s)_A\,{c_5}^{m_s}}{i!\,h^\mu\,(m_s+2\mu+2i)_A}\left(\frac{H}{h}\right)^{2i} \times {}_2F_1\Big(m_s+A, m_s+2\mu+2i; m_s+2\mu+2i+A; 1-c_5\Big)\right\} \tag{25}$$

where $c_5 = \dfrac{(m_s-1)\,\overline{\gamma}}{2\mu h}$.

Proof. Considering an η-μ / inverse gamma composite fading channel, the effective capacity in (8) can be calculated by averaging the SNR, γ, with the PDF given in (24), as follows

$$C_E = -\frac{1}{A}\log_2\left(\frac{2^{2\mu}\mu^{2\mu}\,h^\mu (m_s-1)^{m_s}\overline{\gamma}^{m_s}}{B(m_s,2\mu)}\mathcal{I}_2\right) \tag{26}$$

where

$$\mathcal{I}_2 = \int_0^\infty \frac{(1+\gamma)^{-A}\,\gamma^{2\mu-1}}{{c_4}^{m_s+2\mu}} \times {}_2F_1\left(\frac{m_s+2\mu}{2}, \frac{m_s+2\mu+1}{2}; \mu+\frac{1}{2}; \frac{(2\mu H\gamma)^2}{{c_4}^2}\right). \tag{27}$$

The Gauss hypergeometric function in (27) can be expressed in terms of an infinite series expansion [28, Eq. (07.23.02.0001.01)]. With the aid of [24, Eq. (3.197.9)], the following for the effective capacity can be obtained

$$C_E = -\frac{1}{A}\log_2\left\{\sum_{i=0}^{\infty}\frac{{c_5}^{m_s}\left(\frac{m_s+2\mu}{2}\right)_i\left(\frac{m_s+2\mu+1}{2}\right)_i}{i!\,h^\mu\left(\mu+\frac{1}{2}\right)_i B(m_s,2\mu)}\left(\frac{H}{h}\right)^{2i} \times B\left(m_s+A, 2\mu+2i\right) \times {}_2F_1\Big(m_s+A, m_s+2\mu+2i; m_s+2\mu+2i+A; 1-c_5\Big)\right\}. \tag{28}$$

By expressing the Pochhammer symbol and beta function in terms of the gamma function along with some algebraic manipulations, (28) can be reduced to (25), which completes the proof. □

Proposition 4. *For $\mu, \overline{\gamma}, \theta, B, T \in \mathbb{R}^+$, $m_s > 1$, $\eta \in \mathbb{R}^+$ in Format 1 and $-1 < \eta < 1$ in Format 2, the following closed-form upper bound is valid for the truncation error of* (25)*,*

$$\mathcal{T} \le -\frac{1}{A}\log_2\left\{\frac{(m_s)_A\,{c_5}^{m_s}}{h^\mu\,(c_6)_A}\,{}_1F_0\left(\mu\,;;\left(\frac{H}{h}\right)^2\right) \times {}_2F_1\Big(m_s+A, c_6; c_6+A; 1-c_5\Big)\right\} \tag{29}$$

where $c_6 = m_s + 2\mu + 2p$.

Proof. The truncation error for the infinite series in (25), if it is truncated after $p-1$ terms, is given as

$$\mathcal{T} = -\frac{1}{A}\log_2\left\{\sum_{i=p}^{\infty}\frac{(\mu)_i\,(m_s)_A\,{c_5}^{m_s}}{i!\,h^\mu\,(m_s+2\mu+2i)_A}\left(\frac{H}{h}\right)^{2i} \times {}_2F_1\Big(m_s+A, m_s+2\mu+2i; m_s+2\mu+2i+A; 1-c_5\Big)\right\}. \tag{30}$$

Since the gamma and Gauss hypergeometric functions in (30) are monotonically decreasing with respect to i, $\mathcal{T}$ can be bounded as

$$\mathcal{T} \le -\frac{1}{A}\log_2\left\{{}_2F_1\Big(m_s+A, c_6; c_6+A; 1-c_5\Big) \times \frac{(m_s)_A\,{c_5}^{m_s}}{h^\mu\,(c_6)_A}\sum_{i=p}^{\infty}\frac{(\mu)_i}{i!}\left(\frac{H}{h}\right)^{2i}\right\}. \tag{31}$$

The limits of the summation in (31) can be rewritten as $\sum_{i=p}^{\infty}\frac{(\mu)_i}{i!}\left(\frac{H}{h}\right)^{2i} \le \sum_{i=0}^{\infty}\frac{(\mu)_i}{i!}\left(\frac{H}{h}\right)^{2i}$ as the positive terms are only added up. Notably, (29) can be obtained by applying $\sum_{i=0}^{\infty}\frac{(\mu)_i}{i!}\left(\frac{H}{h}\right)^{2i} = {}_1F_0\left(\mu\,;;\left(\frac{H}{h}\right)^2\right)$. This completes the proof. □

Proposition 5. *For $\mu, \overline{\gamma}, \theta, B, T \in \mathbb{R}^+$, $m_s > 1$, $\eta \in \mathbb{R}^+$ in Format 1 and $-1 < \eta < 1$ in Format 2, and $m_s + 2\mu \gg A$, the effective capacity under η-μ / inverse gamma composite fading conditions can be bounded by the following inequalities*

$$C_E^{UB} < -\frac{1}{A}\log_2\left[\frac{(m_s)_A\,{}_1F_0\left(\mu;;\left(\frac{H}{h}\right)^2\right)}{h^\mu {c_5}^A (m_s+2\mu+2p)_A}\right] \tag{32}$$

and

$$C_E^{LB} > -\frac{1}{A}\log_2\left[\frac{(m_s)_A\,{}_1F_0\left(\mu\,;;\left(\frac{H}{h}\right)^2\right)}{h^\mu {c_5}^A}\right]. \tag{33}$$

Proof. It is evident that $m_s + 2\mu + A \approx m_s + 2\mu$ when $m_s + 2\mu \gg A$ and thus (25) can be tightly upper bounded

$$C_E^{UB} < -\frac{1}{A}\log_2\left\{\sum_{i=0}^{\infty}\frac{(\mu)_i\,(m_s)_A\,{c_5}^{m_s}}{i!\,h^\mu\,(m_s+2\mu+2i)_A}\left(\frac{H}{h}\right)^{2i} \times {}_2F_1\Big(m_s+A, m_s+2\mu+2i; m_s+2\mu+2i; 1-c_5\Big)\right\}. \tag{34}$$

This article has been accepted for publication in a future issue of this journal, but has not been fully edited. Content may change prior to final publication. Citation information: DOI 10.1109/ACCESS.2020.3003207, IEEE Access

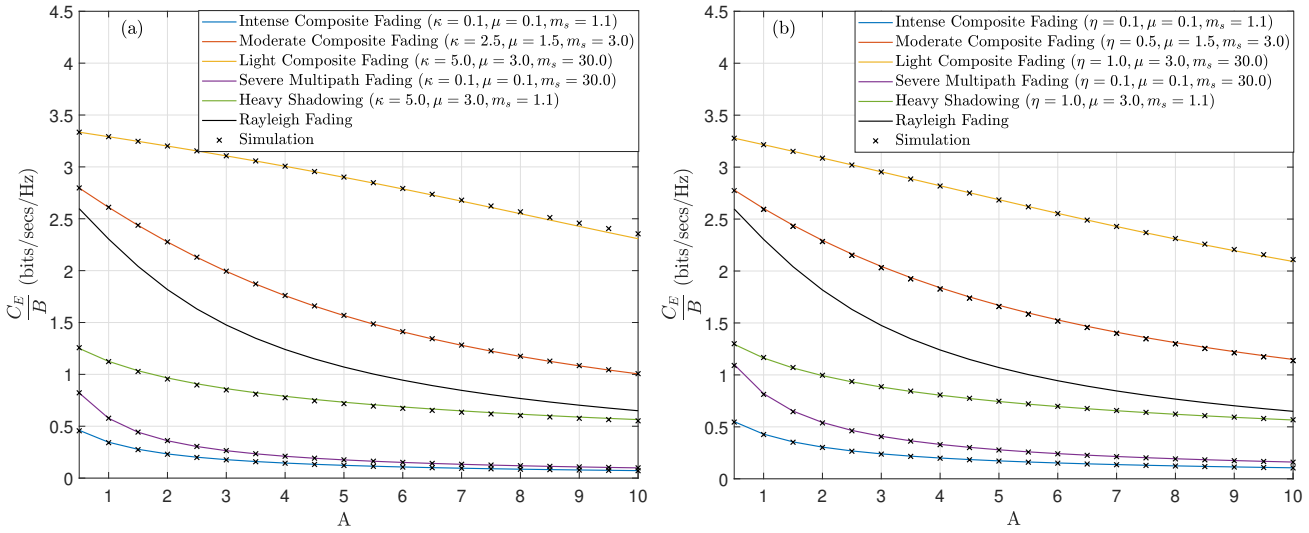

FIGURE 1. C_E/B versus A under (a) κ-μ / inverse gamma and (b) η-μ / inverse gamma composite fading channels with five different combinations of the fading parameters when $\overline{\gamma} = 10$ dB.

Given that ${}_2F_1(m_s + A, m_s + 2\mu + i; m_s + 2\mu + i; 1 - c_5) = {}_1F_0(m_s + A; ; 1 - c_5)$ and by recalling that ${}_1F_0(n; ; 1 + x) \triangleq (-1)^n / x^n$, $n \in \mathbb{R}$, (34) can be reduced as follows

$$C_E^{UB} < -\frac{1}{A}\log_2\left[\frac{(m_s)_A}{h^\mu c_5^A}\sum_{i=0}^{\infty}\frac{(\mu)_i}{i!\,(m_s+2\mu+2i)_A}\left(\frac{H}{h}\right)^{2i}\right]. \tag{35}$$

Using the series representation of ${}_1F_0(\cdot; ; \cdot)$ along with some algebraic manipulations, (35) can be rewritten in closed-form as given in (32). Based on (32) and recalling that $m_s + 2\mu + A \approx m_s + 2\mu$ when $m_s + 2\mu \gg A$, the $(m_s + 2\mu + 2p)_A$ term in (32) can be removed, which yields (33). This completes the proof. □

Proposition 6. *For $\mu, \overline{\gamma}, \theta, B, T \in \mathbb{R}^+$, $m_s > 1$, $\eta \in \mathbb{R}^+$ in Format 1 and $-1 < \eta < 1$ in Format 2 and $\overline{\gamma} \gg 0$, the effective capacity under η-μ / inverse gamma composite fading conditions can be asymptotically expressed as follows*

$$C_E^{asym.} \simeq -\frac{1}{A}\log_2\left\{\frac{1}{h^\mu}{}_1F_0\left(\mu; ; \left(\frac{H}{h}\right)^2\right) \times {}_2F_1\left(A, 2\mu+2p; m_s+2\mu+2p+A; 1-\overline{\gamma}\right)\right\}. \tag{36}$$

Proof. In the high average SNR regime ($\overline{\gamma} \gg 0$), it follows that $\overline{\gamma} \gg 2\mu$, $\overline{\gamma} \gg m_s$ and $\overline{\gamma} \gg A$, namely

$$\frac{(m_s)_A}{(m_s + 2\mu + 2i)_A}\left(\frac{(m_s - 1)\overline{\gamma}}{2\mu h}\right)^{m_s} \simeq \overline{\gamma}^{\,m_s}. \tag{37}$$

With the aid of (37), we can obtain a simple asymptotic expression as given in (36). This completes the proof. □

IV. NUMERICAL RESULTS

The analytic results presented in the previous section are employed to evaluate the corresponding effective capacity in the two generalized composite fading channels while considering different shadowing and multipath fading conditions.

It should noted that we consider only *Format* 1 in the cases of η-μ / inverse gamma composite fading model. Nevertheless, due to the genericness of the derived expressions, numerical results for the corresponding *Format* 2 can be easily deduced. We have also provided the results of some simulations to validate the derived analytic results. In the case of the κ-μ / inverse gamma composite fading model, the simulated sequences were obtained through the straightforward calculation of the ratio of a non-central chi-square RV and a central chi-square RV. In the case of the η-μ / inverse gamma composite fading model, we firstly generated η-μ RVs from κ-μ shadowed RVs using the process presented in [29]. To complete the process, we then multiplied this with an inverse gamma RV. It is worth highlighting that the simulated sequences consisted of 100,000 realizations for both the κ-μ / inverse gamma and η-μ / inverse gamma composite fading models.

Fig. 1 illustrates how the performance of C_E varies as a function of the A parameter over κ-μ / inverse gamma and η-μ / inverse gamma composite fading channels with five different combinations of the respective fading parameters. More specifically, for the κ-μ / inverse gamma composite fading channels, the fading parameters considered are: (i) intense composite fading ($\kappa = 0.1, \mu = 0.1, m_s = 1.1$); (ii) moderate composite fading ($\kappa = 2.5, \mu = 1.5, m_s = 3.0$); (iii) light composite fading ($\kappa = 5.0, \mu = 3.0, m_s = 30.0$); (iv) severe multipath fading ($\kappa = 0.1, \mu = 0.1, m_s = 30.0$); and (v) heavy shadowing ($\kappa = 5.0, \mu = 3.0, m_s = 1.1$). Likewise, for the η-μ / inverse gamma composite fading channels, these are: (i) intense composite fading ($\eta = 0.1, \mu = 0.1, m_s = 1.1$); (ii) moderate composite fading ($\eta = 0.5, \mu = 1.5, m_s = 3.0$); (iii) light composite fading ($\eta = 1.0, \mu = 3.0, m_s = 30.0$); (iv) severe multipath fading

This article has been accepted for publication in a future issue of this journal, but has not been fully edited. Content may change prior to final publication. Citation information: DOI 10.1109/ACCESS.2020.3003207, IEEE Access

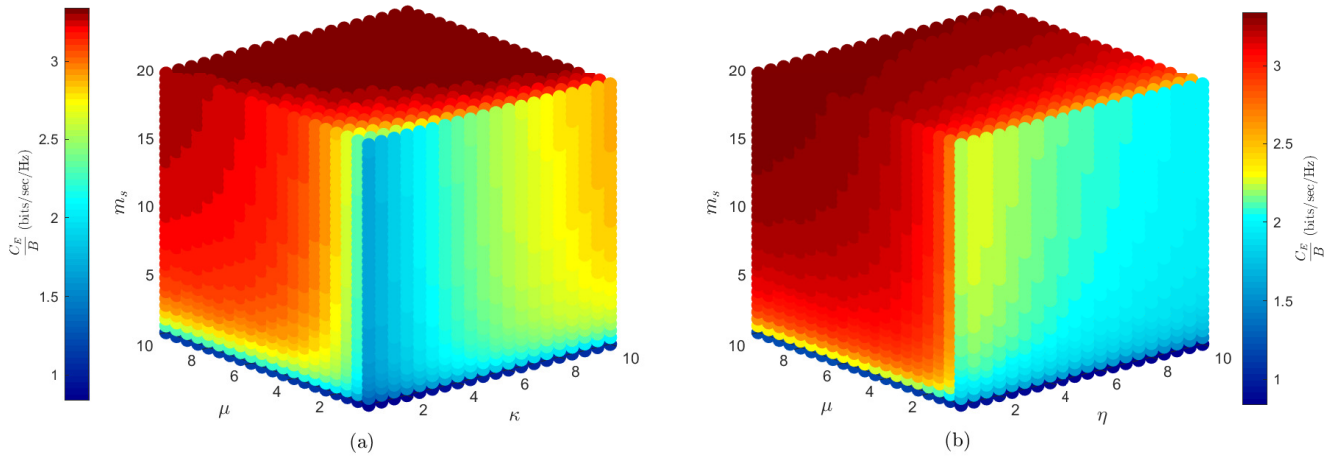

FIGURE 2. C_E/B in a (a) κ-μ / inverse gamma and an (b) η-μ / inverse gamma composite fading channels as a function of their key parameters when $A = 1, \overline{\gamma} = 10$ dB.

$(\eta = 0.1, \mu = 0.1, m_s = 30.0)$; and (v) heavy shadowing $(\eta = 1.0, \mu = 3.0, m_s = 1.1)$. It is worth highlighting that the C_E/B over Rayleigh fading channels is also presented in Fig. 1 for comparison.

It is obvious that the lowest spectral efficiency occurs in the intense composite fading conditions whereas the highest spectral efficiency appears in the light composite fading scenarios. For example, when the channel conditions change from the light composite fading to the intense composite fading at $A = 2$, the achievable spectral efficiency decreases from 3.2 bits/sec/Hz to 0.2 bits/sec/Hz for the κ-μ / inverse gamma composite fading channels whereas this decreases from 3.1 bits/sec/Hz to 0.3 bits/sec/Hz for the η-μ / inverse gamma composite fading channels. Additionally, it is clear that the spectral efficiency is considerably affected by the value of A across all of the considered fading conditions. When comparing the degree of A's effect on the effective capacity for the five different fading conditions, it is observed that the spectral efficiency in the moderate and light composite fading conditions (which are better than those found in a Rayleigh fading environment) is more significantly affected by changes in A compared to those for the rest of the fading conditions (which are worse than those found in a Rayleigh fading environment). For example, when A changes from 0.5 to 10 in κ-μ / inverse gamma composite fading channels, the achievable spectral efficiency decreases from 3.3 bits/sec/Hz to 2.3 bits/sec/Hz in the moderate composite fading conditions whereas in the intense composite fading conditions this only decreases from 0.4 bits/sec/Hz to 0.1 bits/sec/Hz. A similar trend is also observed in η-μ / inverse gamma composite fading channels. For all of the five different fading conditions, the simulated results (shown as symbols in Fig. 1) provided an excellent match to the analytical results presented in Fig. 1.

Fig. 2 shows the performance of the C_E for different parameter values of the two generalized composite fading channels with $A = 1$ and $\overline{\gamma} = 10$ dB. In particular, we varied the parameter values of both such that: $0.5 \leq \kappa \leq 10$; $0.5 \leq \eta \leq 10$; $0.5 \leq \mu \leq 10$; and $1 < m_s \leq 20$. For the κ-μ / inverse gamma composite fading channel, it is clear that the spectral efficiency increases as the κ, μ and m_s parameters become larger, i.e., light composite fading conditions. In contrast, we can observe a decrease in the spectral efficiency when channel undergoes severe multipath fading ($\kappa \to 0.5$, $\mu \to 0.5$) and heavy shadowing ($m_s \to 1$) simultaneously. Similarly, for the η-μ / inverse gamma model, the spectral efficiency increases when there exists light shadowing ($m_s \to 20$) with more multipath clusters ($\mu \to 10$) and when the scattered power of in-phase and quadrature components is identical (i.e., $\eta = 1$). In contrast, the spectral efficiency decreases when channel is subject to intense composite fading (i.e., $\eta \neq 0$, $\mu \to 0.5$, $m_s \to 1$).

Both generalized composite fading models are tremendously versatile as they inherit all of the generality of the κ-μ and η-μ fading models, respectively. Thus, they contain as special cases many of the existing fading models proposed in the open literature. For example, as shown in Fig. 3(a), the κ-μ / inverse gamma model coincides with the Rice fading model when $\mu = 1$, $m_s \to \infty$ and $\kappa = K$ where K is Rice K factor. It is well known that the Rice fading model becomes equivalent to the Rayleigh fading model when $K = 0$. Therefore, when $\mu = 1$, $m_s \to \infty$ and $\kappa = 0$, the κ-μ / inverse gamma model is equivalent to the Rayleigh fading model. Additionally, the Nakagami-m fading model is deduced when $\mu = m$, $m_s \to \infty$ and $\kappa = 0$. Similarly, as shown in Fig. 3(b), the η-μ / inverse gamma composite fading model in *format* 1, corresponds to the Nakagami-q (or Hoyt) fading model ($\eta = q^2$, $\mu = 0.5$ and $m_s \to \infty$), Nakagami-m fading model ($\eta \to 0$, $\mu = m$ and $m_s \to \infty$) and Rayleigh fading model ($\eta \to 0$, $\mu = 1$ and $m_s \to \infty$). As expected, it is shown that the spectral efficiency increases as the average SNR increases (higher $\overline{\gamma}$). Additionally, as shown in Fig. 3, the asymptotic spectral efficiency provides an excellent match to the exact spectral efficiency at high

This article has been accepted for publication in a future issue of this journal, but has not been fully edited. Content may change prior to final publication. Citation information: DOI 10.1109/ACCESS.2020.3003207, IEEE Access

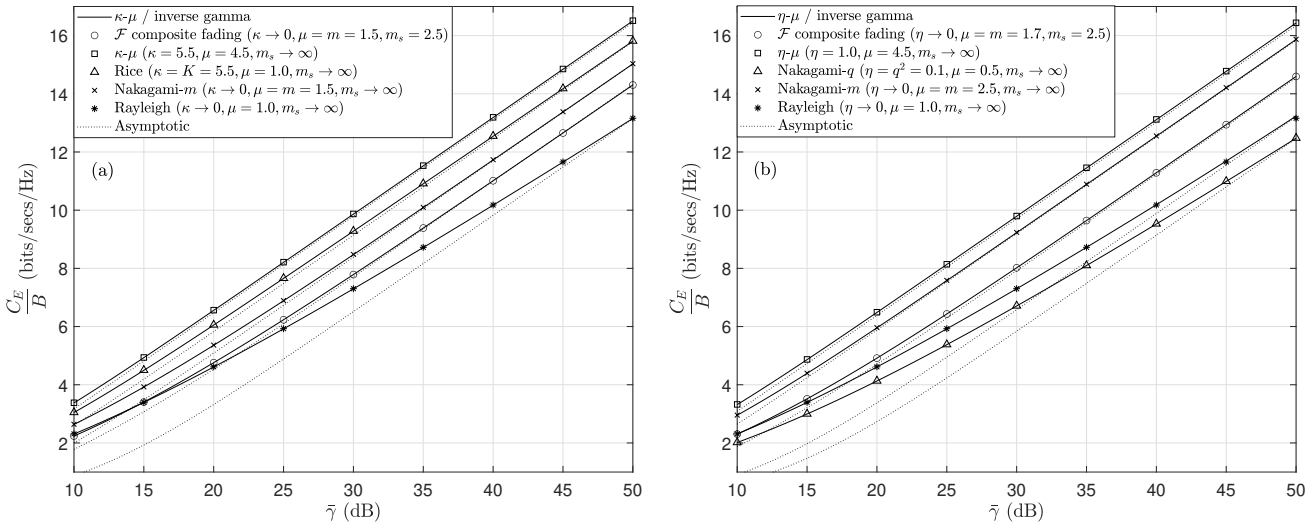

FIGURE 3. C_E/B versus $\overline{\gamma}$ for some special cases of the (a) κ-μ / inverse gamma and (b) η-μ / inverse gamma composite fading channels when $A = 1$.

TABLE 1. Exact, Bounded and Approximated Effective Capacity

A	$\overline{\gamma}$	κ-μ / inverse gamma				η-μ / inverse gamma			
	(dB)	(5)	(13)	(14)	(17)	(22)	(29)	(30)	(33)
0.5	10	2.80	2.86	0.46	2.09	2.78	3.93	0.98	2.59
0.5	30	9.04	9.50	7.11	8.40	9.05	10.58	7.62	9.10
1.0	10	2.61	2.80	0.34	1.94	2.60	3.86	0.86	2.49
1.0	30	8.65	9.45	6.99	8.10	8.73	10.50	7.50	8.97

average SNR levels.

Table I shows the corresponding numerical results of the upper and lower bound, asymptotic and exact representations for moderate composite fading conditions when $A = \{0.5, 1.0\}$ and $\overline{\gamma} = \{10, 30\}$ dB. For the κ-μ / inverse gamma channels, it is shown that the upper bound, i.e., (13), exhibits the most accurate behavior for all of the considered cases with the exception of $A = 1.0$ and $\overline{\gamma} = 30$ dB. On the other hand, for the η-μ / inverse gamma channels, it is found that the approximation, i.e., (33), provides the most accurate behavior for all of the considered cases. Nonetheless, the accuracy of the proposed bounds and approximation is acceptable for all of the considered cases.

V. CONCLUSION

In this paper, accurate analytic expressions for the effective capacity over two generalized composite fading channels have been derived along with simple tight bound representations and approximate expressions. Additionally, the generality of the analytic expressions has been highlighted through reduction to some special cases. Our numerical results have provided important insights into the effect of composite fading conditions and/or delay constraint on the effective capacity of the channels. To validate these numerical results, the results of some simulations have been presented and compared with the numerical results. The proposed bounds and approximate expressions have shown an acceptable level of accuracy and tightness against the exact results, which verifies their usefulness.

REFERENCES

[1] D. Wu and R. Negi, "Effective capacity: a wireless link model for support of quality of service," *IEEE Trans. Wireless Commun.*, vol. 2, no. 4, pp. 630–643, Jul. 2003.

[2] E. A. Jorswieck, R. Mochaourab, and M. Mittelbach, "Effective capacity maximization in multi-antenna channels with covariance feedback," *IEEE Trans. Wireless Commun.*, vol. 9, no. 10, pp. 2988–2993, Oct. 2010.

[3] D. Qiao, M. C. Gursoy, and S. Velipasalar, "Energy efficiency in the low-SNR regime under queueing constraints and channel uncertainty," *IEEE Trans. Commun.*, vol. 59, no. 7, pp. 2006–2017, Jul. 2011.

[4] S. W. Ahn, H. Wang, S. Han, and D. Hong, "The effect of multiplexing users in QoS provisioning scheduling," *IEEE Trans. Veh. Technol.*, vol. 59, no. 5, pp. 2575–2581, Jun. 2010.

[5] L. Musavian, S. Aïssa, and S. Lambotharan, "Effective capacity for interference and delay constrained cognitive radio relay channels," *IEEE Trans. Wireless Commun.*, vol. 9, no. 5, pp. 1698–1707, May 2010.

[6] J. Tang and X. Zhang, "Quality-of-service driven power and rate adaptation over wireless links," *IEEE Trans. Wireless Commun.*, vol. 6, no. 8, pp. 3058–3068, Aug. 2007.

[7] M. Matthaiou, G. C. Alexandropoulos, H. Q. Ngo, and E. G. Larsson, "Analytic framework for the effective rate of MISO fading channels," *IEEE Trans. Commun.*, vol. 60, no. 6, pp. 1741–1751, Jun. 2012.

[8] L. Musavian and S. Aïssa, "Effective capacity of delay-constrained cognitive radio in Nakagami fading channels," *IEEE Trans. Wireless Commun.*, vol. 9, no. 3, pp. 1054–1062, Mar. 2010.

[9] J. Zhang, Z. Tan, H. Wang, Q. Huang, and L. Hanzo, "The effective throughput of MISO systems over κ–μ fading channels," *IEEE Trans. Veh. Technol.*, vol. 63, no. 2, pp. 943–947, Feb. 2014.

[10] J. Zhang, M. Matthaiou, Z. Tan, and H. Wang, "Effective rate analysis of miso η-μ fading channels," in *Proc. IEEE International Conference on Communications (ICC)*, Jun. 2013, pp. 5840–5844.

[11] J. Zhang, L. Dai, Z. Wang, D. W. K. Ng, and W. H. Gerstacker, "Effective rate analysis of MISO systems over α-μ fading channels," in *Proc. IEEE Global Communications Conference (GLOBECOM)*, Dec. 2015, pp. 1–6.

[12] M. You, H. Sun, J. Jiang, and J. Zhang, "Effective rate analysis in Weibull fading channels," *IEEE Wireless Commun. Lett.*, vol. 5, no. 4, pp. 340–343, Aug. 2016.

[13] V. K. Upadhaya, P. S. Chauhan, and S. K. Soni, "Effective capacity analysis over generalized α-η-μ fading channel," in *Proc. International*

Conference on Electrical, Electronics and Computer Engineering (UPCON), Nov. 2019, pp. 1–3.

[14] J. Zhang, L. Dai, W. H. Gerstacker, and Z. Wang, "Effective capacity of communication systems over κ–μ shadowed fading channels," *Electron. Lett.*, vol. 51, no. 19, pp. 1540–1542, Sep. 2015.

[15] S. K. Yoo et al., "A comprehensive analysis of the achievable channel capacity in $\mathcal{F}$ composite fading channels," *IEEE Access*, vol. 7, pp. 34 078–34 094, Feb. 2019.

[16] H. Al-Hmood and H. S. Al-Raweshidy, "Unified approaches based effective capacity analysis over composite α-η-μ / gamma fading channels," *Electron. Lett.*, vol. 54, no. 13, pp. 852–853, Mar. 2018.

[17] F. S. Almehmadi and O. S. Badarneh, "On the effective capacity of Fisher–Snedecor $\mathcal{F}$ fading channels," *Electron. Lett.*, vol. 54, no. 18, pp. 1068–1070, Sep. 2018.

[18] R. Singh and M. Rawat, "On the performance analysis of effective capacity of double shadowed κ-μ fading channels," in *Proc. IEEE Region 10 Conference (TENCON)*, Oct. 2019, pp. 806–810.

[19] X. Li, J. Li, L. Li, J. Jin, J. Zhang, and D. Zhang, "Effective rate of MISO systems over κ-μ shadowed fading channels," *IEEE Access*, vol. 5, pp. 10 605–10 611, Jun. 2017.

[20] S. Chen, J. Zhang, G. K. Karagiannidis, and B. Ai, "Effective rate of MISO systems over Fisher–Snedecor $\mathcal{F}$ fading channels," *IEEE Commun. Lett.*, vol. 22, no. 12, pp. 2619–2622, Dec. 2018.

[21] S. K. Yoo et al., "The κ-μ / inverse gamma and η-μ / inverse gamma composite fading models: Fundamental statistics and empirical validation," *IEEE Trans. Commun.*, Dec. 2017.

[22] S. K. Yoo, S. L. Cotton, P. C. Sofotasios, S. Muhaidat, O. S. Badarneh, and G. K. Karagiannidis, "Entropy and energy detection-based spectrum sensing over $\mathcal{F}$ composite fading channels," *IEEE Trans. Commun.*, vol. 67, no. 7, pp. 4641–4653, Feb. 2019.

[23] M. D. Yacoub, "The κ-μ distribution and the η-μ distribution," *IEEE Antennas Propag. Mag.*, vol. 49, no. 1, pp. 68–81, Feb. 2007.

[24] I. S. Gradshteyn and I. M. Ryzhik, *Table of Integrals, Series, and Products*, 7th ed. London: Academic Press, 2007.

[25] M. Abramowitz and I. A. Stegun, *Handbook of mathematical functions*. National Bureau of Standards, 1972.

[26] S. O. Rice, "*Mathematical analysis of random noise*," Bell System Technical Journal, vol. 24, no. 1, pp. 46–156, Jan. 1945.

[27] J. A. Hanley and B. J. McNeil, "The meaning and use of the area under a receiver operating characteristic (ROC) curve," *Radiology*, vol. 143, no. 1, pp. 29–36, Apr. 1982.

[28] *Wolfram Research, Inc.*, 2019, visited on 12/03/2019. [Online]. Available: http://functions.wolfram.com/id.

[29] L. Moreno-Pozas, F. J. Lopez-Martinez, J. F. Paris, and E. Martos-Naya, "The κ-μ shadowed fading model: Unifying the κ-μ and η-μ distributions," *IEEE Trans. Veh. Technol.*, vol. 65, no. 12, pp. 9630–9641, Dec. 2016.